HHS Public Access

Author manuscript

J Bone Miner Res. Author manuscript; available in PMC 2015 October 01.

Published in final edited form as:

J Bone Miner Res. 2014 October ; 29(10): 2262–2275. doi:10.1002/jbmr.2256.

Epiphyseal chondrocyte secondary ossification centers require thyroid hormone activation of Indian hedgehog and osterix signaling

Weirong Xing[1,2], **Shaohong Cheng**[1], **Jon Wergedal**[1,2], and **Subburaman Mohan**[1,2]

[1]Musculoskeletal Disease Center, Jerry L. Pettis Memorial VA Medical Center, Loma Linda, California, USA

[2]Department of Medicine, Loma Linda University, Loma Linda, California, USA

Abstract

Thyroid hormones (TH) are known to regulate endochondral ossification during skeletal development via acting directly in chondrocytes and osteoblasts. In this study, we focused on TH effects on the secondary ossification center (SOC), since the time of appearance of SOCs in several species coincides with the time when peak levels of TH are attained. Accordingly, μCT evaluation of femurs and tibias at day 21 in TH-deficient and control mice revealed that endochondral ossification of SOCs is severely compromised due to TH deficiency and that TH treatment for 10 days completely rescued this phenotype. Staining of cartilage and bone in the epiphysis revealed that while all of the cartilage is converted into bone in the prepubertal control mice, this conversion failed to occur in the TH-deficient mice. Immunohistochemistry studies revealed that TH treatment of *Tshr*$^{-/-}$ mice induced expression of Ihh and Osx in Col2 expressing chondrocytes in the SOC at day 7 which subsequently differentiate into Col10/osteocalcin expressing chondro-osteoblasts at day 10. Consistent with these data, treatment of tibia cultures from 3-day old mice with10 ng/ml TH increased expression of Osx, Col10, ALP and osteocalcin in the epiphysis by 6–60 fold. Furthermore, knockdown of the TH-induced increase in Osx expression using lentiviral shRNA significantly blocked TH-induced ALP and osteocalcin expression in chondrocytes. Treatment of chondrogenic cells with an Ihh inhibitor abolished chondro-osteoblast differentiation and SOC formation. Our findings indicate that TH regulates the SOC initiation and progression via differentiating chondrocytes into bone matrix producing osteoblasts by stimulating Ihh and Osx expression in chondrocytes.

Correspondence: Subburaman Mohan, Ph.D., Musculoskeletal Disease Center, Jerry L. Pettis Memorial VA Medical Center, 11201 Benton Street (151), Loma Linda, CA 92357, USA. Tel: 1-909-825-7084, Ext 2932. Fax: 1-909-796-1680. Subburaman.mohan@va.gov.

AUTHOR CONTRIBUTIONS

Study design: WX and SM. Acquisition of data: WX, JW and SC. Analysis and interpretation of data: WX and SM. Drafting manuscript: WX and SM. Revising manuscript: WX and SM. Approved final version of manuscript: WX, SC, JW and SM. SM accepts responsibility for integrity of data analysis.

COMPETING FINANICAL INTERESTS

The authors declare no competing financial interests.

Keywords

Osteoblasts; Thyroid hormone; Ossification; Bone formation; Chondrocytes; Hypothyroidism; Differentiation

INTRODUCTION

In mammals, longitudinal skeletal growth of endochondral bones occurs rapidly in embryonic and early postnatal life. Longitudinal growth slows until pubertal growth when the skeletal growth rate again briefly increases (1). Longitudinal skeletal growth is a result of proliferation and differentiation of chondrocytes at the growth plate (2–4). During endochondral ossification, osteoprogenitors inside mesenchymal condensations differentiate into chondrocytes, forming a cartilage template that is subsequently replaced by mineralized bone (2, 5, 6). The perichondrial cells surrounding the cartilage are derived from the differentiation of condensed mesenchymal cells into osteoblasts which contribute to the development of compact bone via an intramembranous bone formation process (2–6). The development of bone from a cartilaginous scaffold involves formation of both a primary ossification center (POC) and a secondary ossification center (SOC). It has been established that POCs form at E15.5 during mouse embryonic development. SOCs normally begin to form sometime later, primarily after birth, around murine postnatal days 5 to 7 (7). It is now generally accepted that the ossification of POCs begins with the formation of a mineralized bony collar around the nascent bone midshaft followed by hypertrophy of the local cartilage, proceeding with invasion of capillaries, calcification of the extracelluar matrix, initiation of osteoclastic cell resorption, and further replacement of the cartilaginous matrix with a bone matrix (2–6). Endochondral ossification at POCs is known to be tightly regulated by the combined actions of a number of growth factors (PTHrp, Ihh, IGF-I, BMP/TGFβ, Wnt, VEGF), and transcription factors (Sox9, Runx2, Osterix, β-catenin) (2–6, 8–12). Dysregulation in the production and/or actions of any of the growth factors that regulate endochondral ossification results in skeletal diseases including chondrodysplasias and osteoarthritis (5, 10, 13).

Both POC and SOC processes involve establishment of growth plates and resorption of cartilage for replacement with bone. However there are important distinctions between them; the timing, the location of the cartilage template, as well as the direction through which ossification proceeds are distinctly different (7, 14, 15). The interaction between Ihh and PTHrp has been considered to play a key role in the transition from pristine cartilage to advancing bone during POC formation (16–18). However, the nature of these and other regulatory molecules, and their signaling pathways, as well as the cellular processes that contribute to the initiation and progression of SOC formation remains poorly understood.

Thyroid hormones (TH), triiodothyronine (**T_3**) and thyroxine (**T_4**), play an important role in normal endochondral ossification during skeletal development, linear growth, maintenance of bone mass and efficient fracture healing (19–22). The major form of thyroid hormone in the blood is T_4, which has a longer half-life than T_3. T_4 is converted to active T_3 within cells by deiodinases (5′-iodinase). Juvenile hypothyroidism causes growth arrest with delayed

bone formation and mineralization while TH replacement induces rapid catch-up growth (19–22). By contrast, childhood thyrotoxicosis accelerates bone formation, with premature closure of the growth plates and skull sutures, leading to short stature and craniosynostosis (19–22). Our recent studies using mice with a combination of TH and growth hormone (GH) deficiencies have provided unequivocal evidence that there is an important window in time, prior to puberty, when the effects of GH are surprisingly small, and that instead TH plays a critical role in the continuing regulation of skeletal development and growth (22). It is of interest that the time of appearance of SOCs in several species including mice, rats, and humans coincides with the time when peak levels of TH are measured (23–28). In humans the identification of proximal humeral epiphyseal secondary ossification centers coincides with the attainment of peak levels of circulating TH, occurring in the late third trimester-early postnatal period (36–42 weeks) (23, 26, 27). Since the postnatal rise of TH in mice occurs between days 5–14, a time of heightened SOC activity, a developmental period considered equivalent to the comparable human late third trimester-early postnatal period (29, 30), it is hypothesized that the rise in TH is a contributing factor to the initiation and progression of secondary ossification in both animals and humans. In this study, we evaluated the role, and mechanism of action, of TH in the initiation and progression of SOC formation in TH deficient mice. Our findings provide the first experimental evidence that the rise in serum TH level during the murine prepubertal growth period (days 5–14) directly initiates SOC activity, by promoting conversion of osterix expressing chondrocytes into bone matrix producing chondro/osteoblasts via a hedgehog signaling pathway.

MATERIALS AND METHODS

Chemicals, recombinant proteins and biological reagents

T3 and T4 were purchased from Sigma (Saint Louis, MO). Pre-made lentiviruses expressing small hairpin RNA (shRNA) specifically against Osx and GFP, and specific antibodies to mouse osterix (Osx) were purchased from Santa Cruz Biotechnology (Santa Cruz, CA). The chondrogenic cell line ATDC5 derived from teratocarcinoma AT805 was purchased from the American Type Culture Collection (Manassas, VA).

Mouse models

Tshr$^{+/-}$ heterozygous mice with a point mutation in the coding region of the thyroid stimulating hormone receptor (*Tshr*) gene was purchased from the Jackson Laboratory (Bar Harbor, Maine). Osterix-cherry reporter mice were kindly provided by Dr. Peter Maye at the University of Connecticut Health Center (31). Both male and female mice in approximately equal numbers were used and the data from both newborn genders were pooled for analyses. Mice were housed at the Jerry L. Pettis Memorial VA Medical Center Veterinary Medical Unit (Loma Linda, CA) under standard approved laboratory conditions. All the procedures were performed with the approval of the Institutional Animal Care and Use Committee of the Jerry L Pettis Memorial VA Medical Center. Mice were anesthetized with approved anesthetics (Isoflurane, ketamine/xylazine) prior to procedures. For euthanasia, animals were exposed to CO_2 prior to cervical dislocation.

Skeleton staining

Alizarin red staining of the long bones from 14 day old *Tshr*$^{-/-}$ and *Tshr*$^{+/-}$ mice was performed using an established method (32).

TH rescue experiments

Tshr$^{-/-}$ mice were injected intraperitoneally with a combination of 1 μg T3 and 10 μg of T4 daily for 10 days from day 5 to day 14 or the same volume of vehicle (5 mM NaOH). Littermate *Tshr*$^{+/-}$ mice treated with vehicle were used as controls. At different times after initiation of T3/T4 treatment, mice were euthanized; bones were removed and used for various analyses.

Histological Analyses

Mouse tibias and femurs were fixed in 10% formalin overnight, washed, decalcified in 10% EDTA (pH 7.4) at 4 °C for 7 days with shaking and embedded in paraffin for sectioning. Consecutive sections of the proximal tibia epiphyses and growth plates were stained with trichrome and Safranin-O, respectively. Two images from 2 longitudinal sections with 5 sections apart from the middle of tibias were taken for quantification. The histological measurements of bone area, total area, growth plate thickness, and hypertrophic region were made as described previously in a blinded fashion with computer software OsteoMeasure (OsteoMetrics, Decatur, GA) (33, 34). An average of two image quantifications per animal was used. The magnification of the images is 40 times (4 × 10 = 40).

Immunohistochemistry analyses

Immunohistochemistry was performed using a rabbit immunohistochemistry kit (Vector Laboratories, Burlingame, CA) according to the manufacturer's instructions. Briefly, consecutive tissue sections were de-paraffinized in histochoice clearing agent, rehydrated in a graded series of ethanol and tap water solutions, and treated with 3% H_2O_2 for 30 minutes to inactivate endogenous peroxidase activity. The sections were then rinsed thoroughly with PBS (pH 7.4) and incubated in 2 mg/ml hyaluronidase (Sigma, St. Louise, MO) (pH7.4) for 30 minutes at 37 °C for epitope recovery. The sections were pretreated with a blocking solution containing normal goat serum for 20 minutes, and then incubated with primary antibodies against Osx, Ihh, osteocalcin, collagen 2 and collagen 10, respectively. Antibody sources and dilutions are described in detail in Supplementary Table 1. Negative control sections were incubated with normal rabbit IgG. After an overnight incubation at 4 °C, the sections were rinsed with PBS, and incubated with biotinylated anti-rat or anti-rabbit secondary antibodies for 30 minutes at room temperature. The sections were then washed in PBS, incubated with VECTASTAIN Elite ABC Reagent for 30 minutes, rinsed again with PBS, and incubated with the Vector Blue or Vector NovaRED substrate until the desired color stain had developed. For double antigen labeling, the Vectorstain kits with different enzyme systems and their substrates, and ImmPRESS reagents were used to label each antigen according to the manufacturer's instruction (Vector Laboratories).

Micro-CT evaluation of the secondary ossification centers

Trabecular bone microarchitecture of the tibia epiphyses (i.e. the secondary ossification centers) isolated from 21 day old mice were assessed by micro-CT (viva CT40, Scanco Medical AG, Switzerland) as described previously (35, 36). The femurs and tibias were fixed in 10% formalin overnight, washed with PBS and immersed in PBS to prevent them from drying. Samples were scanned in phosphate buffered saline (pH 7.4). The X-ray tube potential was 70 kVp for cortical bone and 45 kVp for trabecular bone. Vovel size was 10.5 μm^3. The selected region of interest (ROI) was 1.05 mm of the epiphysis above the growth plate as described in the guidelines (37). To analyze SOC formation, the proximal tibial epiphyses were used for measurement of newly formed bone. Parameters such as bone volume (BV, mm^3), bone volume fraction (BV/TV, %), trabecular number (Tb.N, mm^{-1}), trabecular thickness (Tb.Th, μm) and trabecular space (Tb.Sp, μm) were evaluated as described previously (35–37).

Cell culture

ATDC5 cells were maintained in DMEM/F12 medium containing 10% FBS, penicillin (100 units/ml), and streptomycin (100 μg/ml) as described (38). Cells were incubated in the presence of serum-free DMEM/F12 medium containing 0.1% bovine serum albumin (BSA) and antibiotics for 24 h prior to treatment with T3, vehicle or cyclopamine. At different times, cultures were terminated and used for various analyses.

Nodule assay and ALP staining

ATDC5 cells were maintained in a DMEM-F12 mineralization medium containing 10 mM β-glycerophosphate, 50 μg/ml ascorbic acid and 5% FBS with or without T3 for 7 and 24 days, respectively, prior to staining for ALP activity and mineralized nodules as described (39, 40).

Transduction in chondrogenic cells

For knockdown studies, ATDC5 cells were transduced with pre-made Lenti-viral particles expressing shRNA against mouse Osx or control GFP in 6-well culture plates in the presence of 8 μg/ml of polybrene, as described by the manufacturer. Twenty four hours later, the cells were cultured in a fresh osteoblast differentiation medium and treated with T3 or vehicle, followed by RNA extraction for real-time RT-PCR.

Mouse tibia bone culture

Tibias were surgically isolated from 2-day old C57BL/6 mice and were incubated in serum-free αMEM containing 0.5% BSA, 50 μg/ml ascorbic acid, 1 mM β-glycerol phosphate, 100 units/ml penicillin and 100 μg/ml streptomycin at 37 °C in humidified air with 5% CO_2 as reported (41). T3 (10 ng/ml) or the same volume of vehicle control was added to medium 1 day later, bones were cultured for 10 days for RNA extraction and real-time RT-PCR.

RNA extraction and quantitative PCR

RNA was extracted from ATDC5 cells as described previously (36). Epiphysis and growth plate regions of long bones were isolated and ground to powder in liquid nitrogen using a

mortar and pestle prior to RNA extraction. An aliquot of RNA (25 ng) was reverse-transcribed with an oligo $(dT)_{12–18}$ primer into cDNA in a 20 μl reaction volume. The real time PCR reaction contained 0.5 μl of template cDNA, 1x SYBR GREEN master mix (ABI), and 100 nM of specific forward and reverse primers in a 25 μl reaction volume. Primers for peptidyl prolyl isomerase A (PPIA) was used to normalize the expression data for the genes of interest. The primer sequences used for real-time PCR are listed in supplementary Table 2.

Statistical Analysis

Data are presented as the mean ± standard error of means (SEM) from 6–10 mice from each group. Significant difference was determined as $P \leq 0.05$ or $P \leq 0.01$. Data were analyzed by Student's t-test or two-way ANOVA as appropriate.

RESULTS

TH deficiency in *Tshr* mutant mice impairs epiphysis formation

Alizarin red staining of long bones from 2 week old mice revealed severely impaired mineralization in the epiphyses of *Tshr*$^{-/-}$ mice compared to the littermate controls (Fig. 1A). Micro-CT analyses confirmed impaired mineralization in both tibia and femur epiphyses of *Tshr*$^{-/-}$ mice at ages of 3- and 5-weeks (Fig. 1B, C). The ratio of trabecular (Tb.) bone volume to tissue volume (BV/TV), Tb. number and Tb. thickness were significantly reduced at the proximal epiphysis of the tibias isolated from 3-week old mutant mice as compared to the littermate controls (Fig. 1D, E, F). By contrast, Tb. spacing was dramatically increased in *Tshr*$^{-/-}$ mice (Fig. 1G). The BV/TV, vBMD, and cortical thickness were not significantly changed at the disaphyses of the femur (Supplementary Fig. 1). To evaluate the role of TH in the formation of the epiphysis, we intraperitoneally administered Tshr$^{-/-}$ mice with a combination of 1 μg T3 and 10 μg of T4 or the same volume of vehicle (5 mM NaOH) by daily intraperitoneal injection for 10 days from day 5 to 14. We found that the epiphyseal formation defect of *Tshr*$^{-/-}$ mice was completely rescued by the hormones replacement at a time when TH levels increase (day 5–14) (Fig. 1D, E, F, G).

To determine if TH regulates chondrogenesis and osteogenesis *in vivo*, we examined the histological architecture of cartilage and bone tissue in the growth plate and epiphysis of tibia of *Tshr*$^{+/-}$, *Tshr*$^{-/-}$ and T3/T4 treated *Tshr*$^{-/-}$ mice at different times during postnatal development. We found that there was no bone formation at day 6 in the epiphyses of the tibias in the *Tshr*$^{+/-}$ mice (Supplementary Fig. 2). The cartilage in the epiphyses of the tibias was gradually converted into bone between postnatal day 7 and 21 in the *Tshr*$^{+/-}$ mice that were euthyroid (Fig. 2A, B, C, D, supplementary Fig. 2). However, this conversion of cartilage to bone was severely impaired in the TH deficient, *Tshr*$^{-/-}$ mice. Bone area as well as the ratio of bone area to SOC total area at the proximal tibia epiphysis was greatly reduced in the *Tshr*$^{-/-}$ mutant mice compared to the *Tshr*$^{+/-}$ control mice. Treatment of *Tshr*$^{-/-}$ mice with TH fully rescued the endochondral ossification defect in the epiphyses. Cartilage resorption was drastically reduced in the SOC of the *Tshr*$^{-/-}$ mice, but was restored to a normal level after TH treatment (Fig. 4E). In agreement with the morphological

changes in the epiphyses, the growth plates in *Tshr*$^{-/-}$ mice were thinner than in heterozygous mice (Fig. 2E, F). Both the thicknesses of the growth plate as well as the hypertrophic zone were decreased at day 7, day 10, and day 14 in the *Tshr*$^{-/-}$ mice as compared to heterozygous control mice. Reduction in the thickness of the growth plate and hypertrophic chondrocyte layer were rescued at day 14 with a 10 day treatment of *Tshr*$^{-/-}$ mice with T3/T4.

TH stimulates expression of Ihh and Osx to promote conversion of type 2 collagen expressing chondrocytes into type 10 collagen and osteocalcin expressing chondro/osteoblasts

To study the mechanism for TH-induced endochondral ossification at the epiphyses, we examined the expression levels of key regulators responsible for chondrocyte/osteoblast differentiation, and chondrocyte/osteoblast marker genes in the epiphyses of the proximal tibia of *Tshr*$^{-/-}$ mice and control *Tshr*$^{+/-}$ mice. Immunohistochemistry studies revealed that the expression levels of type 2 collagen (Col2), type 10 collagen (Col10), Indian hedgehog (Ihh), osteocalcin (OC), and osterix (Osx) were comparable between *Tshr*$^{+/-}$ and *Tshr*$^{-/-}$ mice at day 7. However, protein levels of Col10, Ihh, OC and Osx but not Col2 were reduced greatly at day 10 and 14 in the SOC of *Tshr*$^{-/-}$ mice compared to control mice (Fig, 3). The collagen 2 expression remained high at day 10 in the epiphyses of the proximal tibia of *Tshr*$^{-/-}$ mice. TH treatment of *Tshr*$^{-/-}$ mice between days 5–14 rescued the deficiency in the expression levels of Ihh, Osx and OC at day 10 and 14 in Col2 expressing chondrocytes in the SOC. To examine if the TH effect on Ihh induction was direct, we injected *Tshr*$^{-/-}$ mice at day 5 with T3/T4 and evaluated Ihh expression 24 hours later. Figure 4A shows that Ihh expression was increased in epiphyseal chondrocytes of Tshr$^{-/-}$ mice with levels corresponding to those found in euthyroid mice 24 hours after a single injection of T3/T4). Consistent with the immunohistochemistry data, TH injection of osterix-cherry reporter mice at day 5 and 6 caused robust expression of the Osx cherry reporter gene in the SOC at day 10 (Fig. 4B). Interestingly, the Col2 expressing cells at the edge of the SOC expressed high levels of Osx, Col10, and OC at day 10 while the ossification center was forming bone matrix (Fig. 4C). Transcript levels of Osx and OC in the tibia and femurs isolated from *Tshr*$^{-/-}$ mice were reduced compared to the bones from heterozygous control mice, as measured by real-time RT-PCR. (Fig. 4D). Histology analyses revealed reduced expression of TRAP in the SOC of mutant mice (Fig. 4E).

To further examine the genes that are regulated by TH, we extracted total RNA from the epiphyses of 7 day old *Tshr*$^{-/-}$ mice treated with TH or vehicle. Littermates of heterozygous mice treated with vehicle were used as controls. Transcript levels of chondrocyte differentiation markers (Aggrecan and Col10), bone resorption genes (TRAP, MMP13 and MMP14), and osteoblast differentiation markers (OC, ALP and BSP) were significantly down regulated but Col2 and Ctsk remained unchanged in the epiphyses of *Tshr*$^{-/-}$ mice as compared to the corresponding epiphyses of heterozygous control mice (Fig. 5A, B, C, D). Transcription factors (Runx2, Osx, β-catenin, Sox6, Sox9, Gli2 and Mef2C) and extracellular signaling molecules (Ihh, IGF-I, RANKL) were dramatically down regulated in the SOC of *Tshr*$^{-/-}$ mice (Fig. 5E, F, G). TH treatment of *Tshr*$^{-/-}$ mice (day 5 and 6) significantly induced the expression levels of chondro/osteoblast differentiation markers,

bone resorption genes, Ihh, RANKL, Runx2, Osx, Gli1/2, and Mef2C but reduced the expression of Col2, OPG, and Gli3 in the epiphyses. Interestingly, TH replacement of *Tshr*$^{-/-}$ mice did not change the expression levels of Ctsk, PTHrp, β-catenin, and Sox 5/9 in the SOC at day 7. By contrast, expression levels of PTHrp, Sox6 and Sox9 were significantly increased in the epiphyses of *Tshr*$^{-/-}$ mice at day 10 that were rescued by TH treatment during day 5–9 (Supplementary Fig. 3). However, expression levels of Ihh and Osx as well as expression levels of osteoblast marker genes were severely compromised in the epiphyses of *Tshr*$^{-/-}$ mice at day 10. In order to determine the specificity of TH-induced changes in the epiphyses, we also evaluated expression levels of several of the same genes using RNA extracted from growth plates of vehicle treated *Tshr*$^{-/-}$ and *Tshr*$^{+/-}$ mice and TH treated *Tshr*$^{-/-}$ mice. Interestingly, expression levels of Ihh, Sox6, Sox9, Gli1 and Gli2 were significantly upregulated in the growth plates of *Tshr*$^{-/-}$ mice. The expression levels of Col10 and ALP were not altered in *Tshr*$^{-/-}$ mice (Supplementary Fig. 4).

Ihh is one of the key signaling molecules controlling both chondrocyte hypertrophy and bone formation in the developing skeletal system. In order to determine if the TH effect on Ihh expression is direct, we evaluated the effect of TH treatment on expression levels of Ihh and its targets using serum-free tibia cultures derived from 3-day old mice. Treatment with TH for 24 and 72 hours increased the expression of Ihh in the epiphyses by 2- and 12-fold, respectively (Fig. 5H). In fact, TH-induced Ihh expression could be detected at 6 hours after TH treatment (Supplementary Fig. 5). Increased expression of Osx and ALP was observed as early as 24 hours after T3 treatment, and higher levels were reached at 72 hours. The expression of chondro/osteoclast markers, Col10 and OC were significantly increased after 72 hours of TH treatment when Col2 expression was lower. Sox6 expression was reduced at both 24 and 72 hour time points (Fig. 5H).

TH effect on chondro/osteoblast differentiation is dependent on Osx expression

To determine if TH treatment induces differentiation of chondrocytes into chondro/osteoblasts *in vitro*, we cultured ATDC5 chondrogenic cells in an osteoblast differentiation medium containing 50 μg/ml ascorbic acid and 100 mM β-glycophosphate, and treated cells with TH or vehicle for 6 days prior to ALP staining. We found that ALP positive cells were increased by 8-fold upon TH treatment (Fig. 6A). Interestingly, a time-course study found that Osx expression was increased by 3-fold after 24 hours of TH treatment, and remained elevated at day 3 and 7. ALP expression was highest at day 3 while OC expression was highest at day 7 (Fig. 6B). Consistent with these data, 24 day TH treatment of ATDC5 cells in an osteoblast differentiation medium resulted in a significant increase in nodule formation (Fig. 6C). To examine if the increased expression of Osx regulates ATDC5 cell differentiation into chondro/osteoblasts, we transduced ATDC5 cells with lenti-virus expressing shRNA specific to mouse osterix or control GFP. We observed that knockdown of the TH-induced increase in Osx expression significantly blocked TH-induced expression of ALP and OC, and reduced ALP activity in ATDC5 cells (Fig. 6D, E, F, G).

Ihh signaling is required for TH induction of Osx expression and chondro/osteroblast differentiation

To determine if Ihh signaling is involved in regulating TH induction of Osx expression, we examined the effects of cyclopamine, a known inhibitor of hedgehog signaling, on Osx expression in ATDC5 cells. We found that cyclopamine treatment not only blocked the TH-induced increase in Osx, but also the TH effects on the Col10 mRNA level (Supplementary Fig. 6A& C). ALP expression was reduced by 85% in both control and T3 treated cells upon cyclopamine treatment (Supplementary Fig. 6B). To further confirm the role of Ihh signaling in Osx expression, we cultured tibias from 3 day old mice *in vitro* and treated the bones with TH in the presence or absence of cyclopamine for 3 days prior to RNA extraction and real-time PCR. In agreement with ATDC5 cell culture data, we found that suppression of Ihh signaling using cyclopamine abolished Osx, ALP, Col10, Ptch1, and Gli1 expression in primary epithyseal chondrocytes (Fig. 7A, , C, D, E). While treatment of tibia cultures with cyclopamine did not completely abolish TH-induction of OC expression, the expression was reduced from 9 fold to 6 fold (Fig. 7B). Consistent with the *in vitr*o studies, treatment of *Tshr*$^{+/-}$ heterozygous mice with cyclopamine reduced bone volume, trabecular number, but increased trabecular spacing of the tibia epiphyses (Fig. 7E, F, G, H). Thus, our data support that TH regulates SOC initiation and progression via stimulating differentiation of chondrocytes into bone matrix producing osteoblasts by increasing Ihh expression and subsequently Osx expression in epiphyseal chondrocytes.

DISCUSSION

In humans and animals, the postnatal linear skeletal growth rate declines dramatically with age until the pubertal growth spurt when the growth rate briefly increases (1). This deceleration of longitudinal growth in bone during the prepubertal growth period is accompanied by a corresponding increase in the rate of gain in BMD, which is caused by a gradual replacement of cartilage with mineralized bone, at SOCs by an endochondral ossification process, providing the necessary mechanical support for the developing organism (2, 12, 42). While a number of systemic mechanisms involving GH, TH, glucocorticoids, sex hormones, and nutrition have been implicated in regulating SOC endochondral ossification, the key molecular signals that initiate and drive the SOC formation process are unknown. Our data point out that the SOC is severely compromised in TH deficient *Tshr*$^{-/-}$ mice, and that the SOC delay defect is completely rescued by T3/T4 treatment during a window of time when serum levels of TH naturally increase during postnatal growth. Our data provide direct evidence for a key role for circulating TH in the initiation and progression of SOC formation (22).

We and others have shown that TH exerts direct effects on bone cells and that TH deficiency influences development of peak bone mass in both animals and humans (20–22). In this study, we provide the first direct experimental evidence that the rapid increase in TH level that occurs during the second week of postnatal life in mice is obligatory for initiation and progression of SOC activity. The severely compromised bone volume in the epiphysis of *Tshr*$^{-/-}$ mice is completely rescued by TH replacement, administered during postnatal days 5–14, demonstrating that the initiation and progression of endochondral bone formation at

SOC sites is a direct consequence of the increase in TH level, particularly during the prepubertal growth period. In humans, the identification of a proximal humeral epiphyseal ossification center occurs around a gestational age of 38 weeks which also coincides with the attainment of peak circulating level of TH (23, 26, 27), thus predicting a similar role for TH in SOC formation in humans.

While the molecular mechanisms that contribute to the formation of POCs during embryonic development have been extensively investigated, little is known about the cellular processes involved in postnatal SOC development and activity. The prevailing model for endochondral ossification at POCs dictates that proliferating chondrocytes mature into hypertrophic chondrocytes producing mineralized cartilage, and promoting vascularization and remodeling (3, 8, 11, 12, 23, 26, 27, 43–45). Subsequent to the death of chondrocytes, the invading blood vessels are believed to contribute to the source of osteoblast precursors which differentiate into mature osteoblasts and lay down bone matrix (46). However there are important distinctions between POC and SOC activity. POC endochondral bone formation proceeds in a single direction from the center of the diaphysis to the metaphysis with a fairly uniform speed for a relatively long period during primary ossification. By contrast, SOC is known to involve formation of cartilage canals, leading to initiation of ossification in the middle of the epiphysis, which then progresses in a centrifugal-radial pattern during a short period (47, 48). While circulating osteogenic precursors brought in by the invading blood vessels are considered the main source of osteoblasts at the POCs, resting/proliferating chondrocytes surrounding cartilage canals have been proposed to contribute to the development of SOCs in the epiphysis (46, 47). In this regard, *in vitro* experiments have shown that chondrocytes can transdifferentiate into a strictly osteoblast phenotype under appropriate culture conditions (49, 50). Our *in vitro* findings, that treatment of ATDC5 chondrogenic cells with T3 increased expression levels of osteoblast differentiation markers, Osx and OC, suggests that during a unique window of time when TH levels rise rapidly, a subset of chondrocytes in the epiphysis are concurrently converted into chondro/osteoblasts to generate bone matrix.

Previous studies have shown that Osx is required for osteoblast differentiation and bone formation during embryonic development as well as in growing and adult bones (51–53). While these studies focused on the role of Osx expressed in osteoblastic lineage cells in skeletal development, it has recently become known that Osx is also expressed in chondrocytes at certain stages during development and that mice with disruption of Osx in Col2 expressing chondroyctes fail to thrive after birth due to defects in skeletal maturation (54). Consistent with a role for TH-induced Osx in the development of chondro/osteoblasts, Hammond and Schulte-Merker (55) have demonstrated evidence for the presence of Osx positive cells that co-express chondrocyte and osteoblast differentiation markers during certain stages of zebrafish development. Our ongoing studies on the conditional disruption of the Osx gene in chondrocytes during the postnatal growth period provides a plausible causative role for Osx in mediating TH effects on chondro/osteoblast development, and the subsequent ossification at the epiphyses.

When T3/T4 levels are low or absent, the epiphyseal chondrocytes maintain a proliferative state and produce high levels of Col2 as revealed by the time course studies on Safranin-O

staining of the epiphyses of vehicle treated *Tshr*$^{+/-}$ mice and vehicle and T3/T4 treated *Tshr*$^{-/-}$ mice. During early the postnatal growth period in mice, expression levels of transcription factors Sox5, Sox6 and Sox9, the trio that are required for maintaining the chondrocytes in the proliferative state (56), are maintained at relatively high levels. As serum levels of T3/T4 reach a peak during the second week of the postnatal growth period in mice, expression levels of Sox6 decline, while Ihh expression increases markedly, in the epiphysis. Furthermore, expression levels of hypertrophic chondrocyte (Col10) and osteoblast (OC, BSP) markers are increased in epiphyseal chondrocytes. Accordingly, treatment of tibia cultures with T3 stimulated a significant increase in the expression of Ihh but decreased expression Sox6 72 hours after treatment. Thus, the prepubertal rise in TH production is associated with an upregulation of Ihh and Osx signaling and promotion of expression of markers of differentiated osteoblasts in the epiphyseal chondrocytes.

A mechanism of action for the TH effect on Osx expression in chondrocytes could include both direct and indirect influences via regulation of other molecules. A recent study identified a functional TRE in the distal promoter of Ihh that is well conserved among mice, rats and humans (57). Furthermore, this study also identified the Ihh gene as being directly regulated by TH, as its expression is increased by TH treatment in the liver (57). In the mouse Ihh promoter, an everted repeat TRE with 6 nucleotide spacing (5′-TGACCT*ttatgc*AAGTCA-3′) is located from −5766 to −5783 upstream of transcription start site. A similar native TRE sequence (5′-TGACCC*cagctg*GGTCA-3′) derived from the chicken lysozyme promoter has been shown to interact with T3 receptor beta (T3Rβ) as a homodimer or a heterodimer with RXR (58). The receptors bound to TRE containing promoter can recruit chromatin remodeling factors and interact directly with the basic transcriptional machinery to decompact chromatin and activate target gene transcription (59). Ihh exerts its biological activity by altering the balance between full length Gli activator (Gli^A) and truncated Gli repressor (Gli^R). Increased Gli^A and decreased Gli^R expression indicate Hedgehog pathway activation (60). In vertebrates, Gli^A activity is mostly derived from Gli2 while Gli^R function is primarily derived from Gli3. Our observed changes in Gli2 and Gli3 expression in SOCs of TH deficient and euthyroid mice are consistent with TH activation of Ihh signaling in the SOC. To explore this possibility we evaluated whether TH's effect on Osx expression is mediated via Ihh. Accordingly, we found that inhibition of Ihh signaling with cyclopamine blocked the TH-induced increase in Osx expression, as well as the increase in bone-specific marker expression in chondrocytes. Consistent with these data, cyclopamine treatment *in vivo* significantly decreased bone volume in the epiphysis of the tibia of euthyroid *Tshr*$^{+/-}$ mice, thus suggesting that the TH-induced increase in Ihh signaling is a key mediator of the TH effects on Osx expression and secondary ossification.

TRα1 and TRβ1 are expressed in reserve and proliferating chondrocytes in the growth plate, suggesting these cells are direct targets of T3 action. The mechanisms of T3 action in the skeleton have been investigated using mouse models with disruption of ligand binding TRα1 and TRβ1 receptors and knock-in mutations for TRα or TRβ that produce severe resistance to T3 actions (61) TRα1 is the major TR expressed in bone cells and disruption of TRα1 expression impairs bone formation and reduces peak bone mass, thus suggesting that

TRα1 is responsible for the anabolic effects of T3 in bone (61). TRα null mice exhibit wider growth plates and delayed secondary ossification centers at postnatal day 21 (61–63). By contrast, TRβ knockout mice which lack all TRβ isoforms display features of skeletal hyperthyroidism with persistent short stature, advanced endochondral ossification and increased bone mineralization due to accelerated growth plate chondrocyte differentiation (61–63). Growth plates of TRβ knockout mice were narrow and exhibit advanced secondary ossification centers. A recent clinical study demonstrated that a patient who is heterozygous for a *de novo* TRα mutation exhibited growth retardation and femoral epiphyseal dysgenesis despite near-normal TH levels (64). While these studies suggest that TRα and TRβ may exhibit different effects on chondrocyte differentiation and endochondral ossification, additional studies are needed to evaluate the role of various TRs in initiation and progression of SOC at the epiphyses.

A key early event in SOC formation is removal of cartilaginous matrix for replacement in bone matrix. In this regard, expression of MMPs, notably, MMP13 and MMP14, have been detected in the epiphysis and have been shown to play a key role in eroding epiphyseal cartilage (65, 66). We, therefore, asked the question whether TH is involved in regulating expression of MMPs in epiphyseal chondrocytes. We found that expression levels of both MMP13 and MMP14 were decreased in the epiphysis of $Tshr^{-/-}$ mice that were rescued by treatment with TH. By contrast, the expression level of Ctsk, a marker of differentiated osteoclasts, was not affected. Furthermore, T3 treatment caused a significant increase in MMP13 in the epiphysis of serum-free tibia cultures. It remains to be determined whether the TH effect on MMP expression is directly or indirectly mediated via the TH effect on RANKL/OPG expression in epiphyseal chondrocytes.

Based on our data, we conclude that the rapid increase in TH levels during the prepubertal growth period in mice acts directly on epiphyseal chondrocytes modulating expression of key growth factors, altering the activity of transcription factors inhibiting Col2 expression, promoting secretion of enzymes for cartilaginous matrix removal, and by influencing the expression of osteoblast marker proteins involved in actively mineralizing the receptive bone cartilage (Fig. 8). Furthermore our data strongly implicates epiphyseal chondrocytes themselves as being independently capable of carrying out many of these processes. Thus, our data challenges the existing paradigm that similar mechanisms are operative in the POC and SOC processes. Our data indicate that the conversion of chondrocytes into chondro/osteoblasts may occur only during secondary ossification when TH levels rise.

Supplementary Material

Refer to Web version on PubMed Central for supplementary material.

Acknowledgments

We thank Sheila Pourteymoor, Heather Davidson, Catrina Alarcon, Nancy Lowen and Joe Rung-Aroon for technical assistance. We thank Dr. Peter Maye at the University of Connecticut Health Center for providing us the Osterix-cherry reporter mice, and Dr. Donna Strong for proofreading the manuscript. This research was supported by National Institutes of Health Grant AR 048139 to SM. The research work was performed at facilities provided by the Department of Veterans Affairs.

References

1. Lui JC, Baron J. Mechanisms limiting body growth in mammals. Endocr Rev. 2011; 32(3):422–40. [PubMed: 21441345]
2. Mackie EJ, Tatarczuch L, Mirams M. The growth plate chondrocyte and endochondral ossification. J Endocrinol. 2011; 211:109–21. [PubMed: 21642379]
3. Nilsson O, Marino R, De Luca F, Phillip M, Baron J. Endocrine regulation of the growth plate. Horm Res. 2005; 64(4):157–65. [PubMed: 16205094]
4. van der Eerden BC, Karperien M, Wit JM. Systemic and local regulation of the growth plate. Endocr Rev. 2003; 24(6):782–801. [PubMed: 14671005]
5. Long F, Ornitz DM. Development of the endochondral skeleton. Cold Spring Harb Perspect Biol. 2013; 5(1):a008334. [PubMed: 23284041]
6. Zuscik MJ, Hilton MJ, Zhang X, Chen D, O'Keefe RJ. Regulation of chondrogenesis and chondrocyte differentiation by stress. J Clin Invest. 2008; 118(2):429–38. [PubMed: 18246193]
7. Dao DY, Jonason JH, Zhang Y, Hsu W, Chen D, Hilton MJ, et al. Cartilage-specific beta-catenin signaling regulates chondrocyte maturation, generation of ossification centers, and perichondrial bone formation during skeletal development. J Bone Miner Res. 2012; 27(8):1680–94. [PubMed: 22508079]
8. Adams SL, Cohen AJ, Lassova L. Integration of signaling pathways regulating chondrocyte differentiation during endochondral bone formation. J Cell Physiol. 2007; 213(3):635–41. [PubMed: 17886256]
9. Chung UI, Schipani E, McMahon AP, Kronenberg HM. Indian hedgehog couples chondrogenesis to osteogenesis in endochondral bone development. J Clin Invest. 2001; 107(3):295–304. [PubMed: 11160153]
10. Lefebvre V, Smits P. Transcriptional control of chondrocyte fate and differentiation. Birth Defects Res C Embryo Today. 2005; 75(3):200–12. [PubMed: 16187326]
11. Maeda Y, Nakamura E, Nguyen MT, Suva LJ, Swain FL, Razzaque MS, et al. Indian Hedgehog produced by postnatal chondrocytes is essential for maintaining a growth plate and trabecular bone. Proc Natl Acad Sci U S A. 2007; 104(15):6382–7. [PubMed: 17409191]
12. Yang Y. Skeletal morphogenesis during embryonic development. Crit Rev Eukaryot Gene Expr. 2009; 19(3):197–218. [PubMed: 19883365]
13. Staines KA, Pollard AS, McGonnell IM, Farquharson C, Pitsillides AA. Cartilage to bone transitions in health and disease. J Endocrinol. 2013; 219(1):R1–R12. [PubMed: 23959079]
14. Akiyama H, Lefebvre V. Unraveling the transcriptional regulatory machinery in chondrogenesis. J Bone Miner Metab. 2012; 29(4):390–5. [PubMed: 21594584]
15. Cole HA, Yuasa M, Hawley G, Cates JM, Nyman JS, Schoenecker JG. Differential development of the distal and proximal femoral epiphysis and physis in mice. Bone. 2013; 52(1):337–46. [PubMed: 23079139]
16. Kobayashi T, Chung UI, Schipani E, Starbuck M, Karsenty G, Katagiri T, et al. PTHrP and Indian hedgehog control differentiation of growth plate chondrocytes at multiple steps. Development. 2002; 129(12):2977–86. [PubMed: 12050144]
17. Kobayashi T, Soegiarto DW, Yang Y, Lanske B, Schipani E, McMahon AP, et al. Indian hedgehog stimulates periarticular chondrocyte differentiation to regulate growth plate length independently of PTHrP. J Clin Invest. 2005; 115(7):1734–42. [PubMed: 15951842]
18. Kronenberg HM. Developmental regulation of the growth plate. Nature. 2003; 423(6937):332–6. [PubMed: 12748651]
19. Gogakos AI, Duncan Bassett JH, Williams GR. Thyroid and bone. Arch Biochem Biophys. 2010; 503(1):129–36. [PubMed: 20599658]
20. Kim H-Y, Mohan S. Role and mechanisms of actions of thyroid hormone on the skeletal development. Bone Res. 2013; 1(2):146–61.
21. Wojcicka A, Bassett JH, Williams GR. Mechanisms of action of thyroid hormones in the skeleton. Biochim Biophys Acta. 2012; 1830(7):3979–86. [PubMed: 22634735]

22. Xing W, Govoni K, Donahue LR, Kesavan C, Wergedal J, Long C, et al. Genetic evidence that thyroid hormone is indispensable for prepubertal IGF-I expression and bone acquisition in mice. J Bone Miner Res. 2012
23. Brown RS. Minireview: developmental regulation of thyrotropin receptor gene expression in the fetal and newborn thyroid. Endocrinology. 2004; 145(9):4058–61. [PubMed: 15231704]
24. Hernandez A, Martinez ME, Fiering S, Galton VA, St Germain D. Type 3 deiodinase is critical for the maturation and function of the thyroid axis. J Clin Invest. 2006; 116(2):476–84. [PubMed: 16410833]
25. Hood, RD. Developmental and reproductive toxicology: A practical approach. CRC Press; Boca Raton, FL: 2006. Age of appearance and fusion of secondary ossification centers in the humerus and femur.
26. Hume R, Simpson J, Delahunty C, van Toor H, Wu SY, Williams FL, et al. Human fetal and cord serum thyroid hormones: developmental trends and interrelationships. J Clin Endocrinol Metab. 2004; 89(8):4097–103. [PubMed: 15292353]
27. Mahony BS, Bowie JD, Killam AP, Kay HH, Cooper C. Epiphyseal ossification centers in the assessment of fetal maturity: sonographic correlation with the amniocentesis lung profile. Radiology. 1986; 159(2):521–4. [PubMed: 3515425]
28. van der Heide D, Ende-Visser MP. T4, T3 and reverse T3 in the plasma of rats during the first 3 months of life. Acta Endocrinol (Copenh). 1980; 93(4):448–54. [PubMed: 7386115]
29. Noel M, Norris EH, Strickland S. Tissue plasminogen activator is required for the development of fetal alcohol syndrome in mice. Proc Natl Acad Sci U S A. 2011; 108(12):5069–74. [PubMed: 21383198]
30. Scheepens A, van de Waarenburg M, van den Hove D, Blanco CE. A single course of prenatal betamethasone in the rat alters postnatal brain cell proliferation but not apoptosis. J Physiol. 2003; 552(Pt 1):163–75. [PubMed: 12909684]
31. Strecker S, Fu Y, Liu Y, Maye P. Generation and characterization of Osterix-Cherry reporter mice. Genesis. 2013; 51(4):246–58. [PubMed: 23180553]
32. McLeod MJ. Differential staining of cartilage and bone in whole mouse fetuses by alcian blue and alizarin red S. Teratology. 1980; 22(3):299–301. [PubMed: 6165088]
33. Beamer WG, Donahue LR, Rosen CJ, Baylink DJ. Genetic variability in adult bone density among inbred strains of mice. Bone. 1996; 18(5):397–403. [PubMed: 8739896]
34. Qin X, Wergedal JE, Rehage M, Tran K, Newton J, Lam P, et al. Pregnancy-associated plasma protein-A increases osteoblast proliferation in vitro and bone formation in vivo. Endocrinology. 2006; 147(12):5653–61. [PubMed: 16946002]
35. Xing W, Pourteymoor S, Mohan S. Ascorbic acid regulates osterix expression in osteoblasts by activation of prolyl hydroxylase and ubiquitination-mediated proteosomal degradation pathway. Physiol Genomics. 2011; 43(12):749–57. [PubMed: 21467157]
36. Xing W, Kim J, Wergedal J, Chen ST, Mohan S. Ephrin B1 regulates bone marrow stromal cell differentiation and bone formation by influencing TAZ transactivation via complex formation with NHERF1. Mol Cell Biol. 2010; 30(3):711–21. [PubMed: 19995908]
37. Bouxsein ML, Boyd SK, Christiansen BA, Guldberg RE, Jepsen KJ, Muller R. Guidelines for assessment of bone microstructure in rodents using micro-computed tomography. J Bone Miner Res. 2010; 25(7):1468–86. [PubMed: 20533309]
38. Shukunami C, Ishizeki K, Atsumi T, Ohta Y, Suzuki F, Hiraki Y. Cellular hypertrophy and calcification of embryonal carcinoma-derived chondrogenic cell line ATDC5 in vitro. J Bone Miner Res. 1997; 12(8):1174–88. [PubMed: 9258747]
39. Xing W, Baylink D, Kesavan C, Mohan S. HSV-1 amplicon-mediated transfer of 128-kb BMP-2 genomic locus stimulates osteoblast differentiation in vitro. Biochem Biophys Res Commun. 2004; 319(3):781–6. [PubMed: 15184051]
40. Xing W, Singgih A, Kapoor A, Alarcon CM, Baylink DJ, Mohan S. Nuclear factor-E2-related factor-1 mediates ascorbic acid induction of osterix expression via interaction with antioxidant-responsive element in bone cells. J Biol Chem. 2007; 282(30):22052–61. [PubMed: 17510056]

41. Mukherjee A, Rotwein P. Insulin-like growth factor-binding protein-5 inhibits osteoblast differentiation and skeletal growth by blocking insulin-like growth factor actions. Mol Endocrinol. 2008; 22(5):1238–50. [PubMed: 18292241]
42. Richman C, Kutilek S, Miyakoshi N, Srivastava AK, Beamer WG, Donahue LR, et al. Postnatal and pubertal skeletal changes contribute predominantly to the differences in peak bone density between C3H/HeJ and C57BL/6J mice. J Bone Miner Res. 2001; 16(2):386–97. [PubMed: 11204439]
43. Day TF, Yang Y. Wnt and hedgehog signaling pathways in bone development. J Bone Joint Surg Am. 2008; 90 (Suppl 1):19–24. [PubMed: 18292352]
44. Hu H, Hilton MJ, Tu X, Yu K, Ornitz DM, Long F. Sequential roles of Hedgehog and Wnt signaling in osteoblast development. Development. 2005; 132(1):49–60. [PubMed: 15576404]
45. Lefebvre V, Bhattaram P. Vertebrate skeletogenesis. Curr Top Dev Biol. 2010; 90:291–317. [PubMed: 20691853]
46. Maes C, Kobayashi T, Selig MK, Torrekens S, Roth SI, Mackem S, et al. Osteoblast precursors, but not mature osteoblasts, move into developing and fractured bones along with invading blood vessels. Dev Cell. 2010; 19(2):329–44. [PubMed: 20708594]
47. Alvarez J, Costales L, Lopez-Muniz A, Lopez JM. Chondrocytes are released as viable cells during cartilage resorption associated with the formation of intrachondral canals in the rat tibial epiphysis. Cell Tissue Res. 2005; 320(3):501–7. [PubMed: 15846519]
48. Delgado-Baeza E, Nieto-Chaguaceda A, Miralles-Flores C, Santos-Alvarez I. Cartilage canal growth: experimental approach in the rat tibia. Acta Anat (Basel). 1992; 145(2):143–8. [PubMed: 1441886]
49. Descalzi Cancedda F, Gentili C, Manduca P, Cancedda R. Hypertrophic chondrocytes undergo further differentiation in culture. J Cell Biol. 1992; 117(2):427–35. [PubMed: 1560033]
50. Roach HI, Erenpreisa J, Aigner T. Osteogenic differentiation of hypertrophic chondrocytes involves asymmetric cell divisions and apoptosis. J Cell Biol. 1995; 131(2):483–94. [PubMed: 7593173]
51. Baek WY, Lee MA, Jung JW, Kim SY, Akiyama H, de Crombrugghe B, et al. Positive regulation of adult bone formation by osteoblast-specific transcription factor osterix. J Bone Miner Res. 2009; 24(6):1055–65. [PubMed: 19113927]
52. Nakashima K, Zhou X, Kunkel G, Zhang Z, Deng JM, Behringer RR, et al. The novel zinc finger-containing transcription factor osterix is required for osteoblast differentiation and bone formation. Cell. 2002; 108(1):17–29. [PubMed: 11792318]
53. Zhou X, Zhang Z, Feng JQ, Dusevich VM, Sinha K, Zhang H, et al. Multiple functions of Osterix are required for bone growth and homeostasis in postnatal mice. Proc Natl Acad Sci U S A. 2010; 107(29):12919–24. [PubMed: 20615976]
54. Cheng S, Xing W, Zhou X, Mohan S. Haploinsufficiency of osterix in chondrocytes impairs skeletal growth in mice. Physiol Genomics. 2013; 45(19):917–23. [PubMed: 23943855]
55. Hammond CL, Schulte-Merker S. Two populations of endochondral osteoblasts with differential sensitivity to Hedgehog signalling. Development. 2009; 136(23):3991–4000. [PubMed: 19906866]
56. Leung VY, Gao B, Leung KK, Melhado IG, Wynn SL, Au TY, et al. SOX9 governs differentiation stage-specific gene expression in growth plate chondrocytes via direct concomitant transactivation and repression. PLoS Genet. 7(11):e1002356. [PubMed: 22072985]
57. Paquette MA, Dong H, Gagne R, Williams A, Malowany M, Wade MG, et al. Thyroid hormone-regulated gene expression in juvenile mouse liver: identification of thyroid response elements using microarray profiling and in silico analyses. BMC Genomics. 2011; 12:634. [PubMed: 22206413]
58. Nelson CC, Hendy SC, Faris JS, Romaniuk PJ. The effects of P-box substitutions in thyroid hormone receptor on DNA binding specificity. Mol Endocrinol. 1994; 8(7):829–40. [PubMed: 7984145]
59. Aranda A, Pascual A. Nuclear hormone receptors and gene expression. Physiological reviews. 2001; 81(3):1269–304. [PubMed: 11427696]
60. Ingham PW, McMahon AP. Hedgehog signaling in animal development: paradigms and principles. Genes Dev. 2001; 15(23):3059–87. [PubMed: 11731473]

61. Wojcicka A, Bassett JH, Williams GR. Mechanisms of action of thyroid hormones in the skeleton. Biochim Biophys Acta. 2013; 1830(7):3979–86. [PubMed: 22634735]

62. O'Shea PJ, Bassett JH, Sriskantharajah S, Ying H, Cheng SY, Williams GR. Contrasting skeletal phenotypes in mice with an identical mutation targeted to thyroid hormone receptor alpha1 or beta. Mol Endocrinol. 2005; 19(12):3045–59. [PubMed: 16051666]

63. Bassett JH, O'Shea PJ, Sriskantharajah S, Rabier B, Boyde A, Howell PG, et al. Thyroid hormone excess rather than thyrotropin deficiency induces osteoporosis in hyperthyroidism. Mol Endocrinol. 2007; 21(5):1095–107. [PubMed: 17327419]

64. Bochukova E, Schoenmakers N, Agostini M, Schoenmakers E, Rajanayagam O, Keogh JM, et al. A mutation in the thyroid hormone receptor alpha gene. N Engl J Med. 2012; 366(3):243–9. [PubMed: 22168587]

65. Holmbeck K, Bianco P, Caterina J, Yamada S, Kromer M, Kuznetsov SA, et al. MT1-MMP-deficient mice develop dwarfism, osteopenia, arthritis, and connective tissue disease due to inadequate collagen turnover. Cell. 1999; 99(1):81–92. [PubMed: 10520996]

66. Inada M, Wang Y, Byrne MH, Rahman MU, Miyaura C, Lopez-Otin C, et al. Critical roles for collagenase-3 (Mmp13) in development of growth plate cartilage and in endochondral ossification. Proc Natl Acad Sci U S A. 2004; 101(49):17192–7. [PubMed: 15563592]

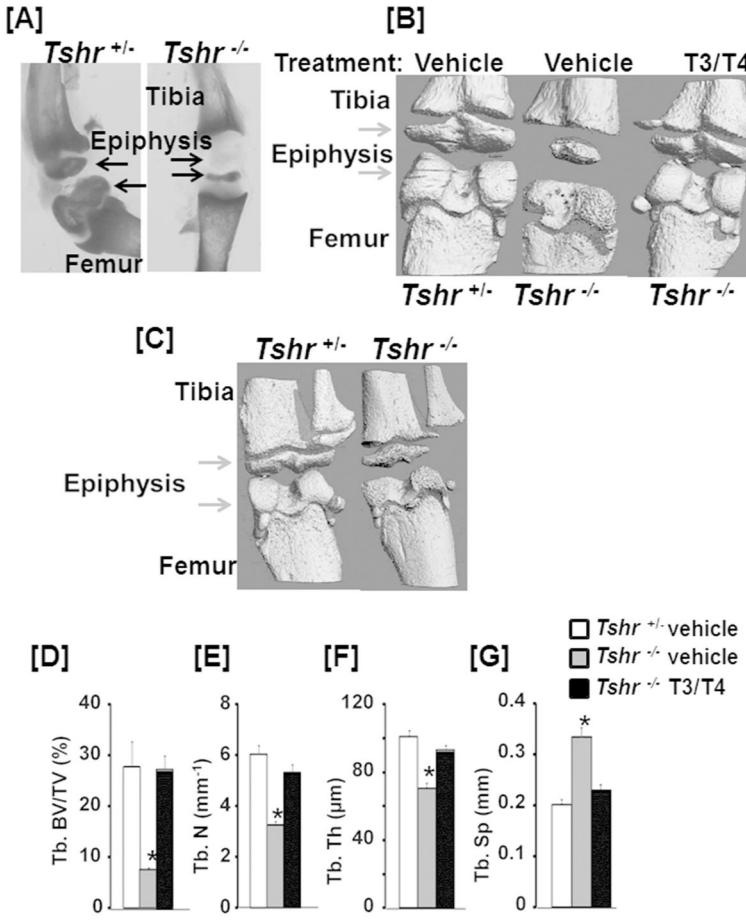

Figure 1. TH deficiency in *Tshr*$^{-/-}$ mice impairs epiphysis formation

Alizarin red stained [**A**] and micro-CT [**B, C**] images of long bones of 2 week [**A**], 3 week [B] or 5 week [**C**] old TH deficient *Tshr*$^{-/-}$ and *Tshr*$^{+/-}$ control mice. Arrowheads indicate epiphysis defects of the *Tshr*$^{-/-}$ tibia and femur as compared to the control bones from *Tshr*$^{+/-}$ mice. [**D-G**] Quantitative micro-CT data of the trabecular bone volume to total volume (Tb. BV/TV), trabecular number (Tb. N), trabecular thickness (Tb. Th), and trabecular spacing (Tb. Sp) of the tibia epiphyses of 3 week old vehicle or TH treated *Tshr*$^{-/-}$ mice and vehicle treated *Tshr*$^{+/-}$ control mice. Values are mean ± SEM (N = 5). The asterisk indicates a significant difference (P<0.01) in *Tshr*$^{-/-}$ mice treated with vehicle compared to TH treated *Tshr*$^{-/-}$ or vehicle treated *Tshr*$^{+/-}$ mice. Formation of the epiphysis both in the tibia and femur are severely compromised in TH deficient *Tshr*$^{-/-}$ mice and epiphyseal defects in *Tshr*$^{-/-}$ mice are completely rescued by 10 day treatment with TH.

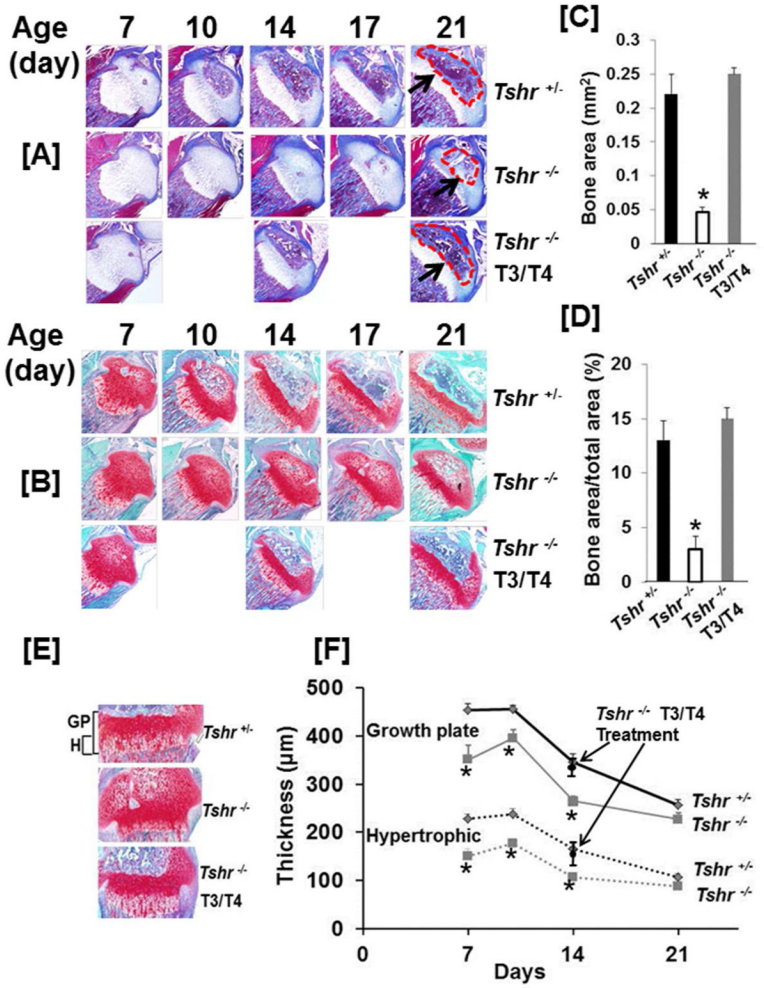

Figure 2. TH is essential for initiation and progression of endochondral ossification

Trichrome [**A**] and Safranin-O [**B**] stained sections of proximal tibial epiphyses at different times during postnatal growth. Arrows and dashed regions indicate the SOC of 21 day old tibia from *Tshr*$^{+/-}$ control mice and *Tshr*$^{-/-}$ mice treated with vehicle or T3/T4. **[C & D]** Amount of bone in the epiphyses of vehicle treated *Tshr*$^{+/-}$, *Tshr*$^{-/-}$ and TH treated Tshr$^{-/-}$ mice in the trichrome stained sections measured by histology. **[E]** Safranin-O stained growth plates from vehicle treated *Tshr*$^{+/-}$, *Tshr*$^{-/-}$ and TH treated Tshr$^{-/-}$ mice. **[F]** Thickness of growth plates and hypertrophic regions of vehicle treated *Tshr*$^{+/-}$, *Tshr*$^{-/-}$ and TH treated Tshr$^{-/-}$ mice. The asterisk indicates a significant difference ($P<0.01$) in *Tshr*$^{-/-}$ mice treated with vehicle compared to TH treated *Tshr*$^{-/-}$ or vehicle treated *Tshr*$^{+/-}$ mice. Replacement of cartilage into bone at the tibial epiphyses of *Tshr*$^{-/-}$ mice is severely compromised but fully rescued by 10 day treatment with TH during postnatal growth when TH levels rise in mice. Chondrocyte hypertrophy at the growth plate is also significantly impaired by TH deficiency.

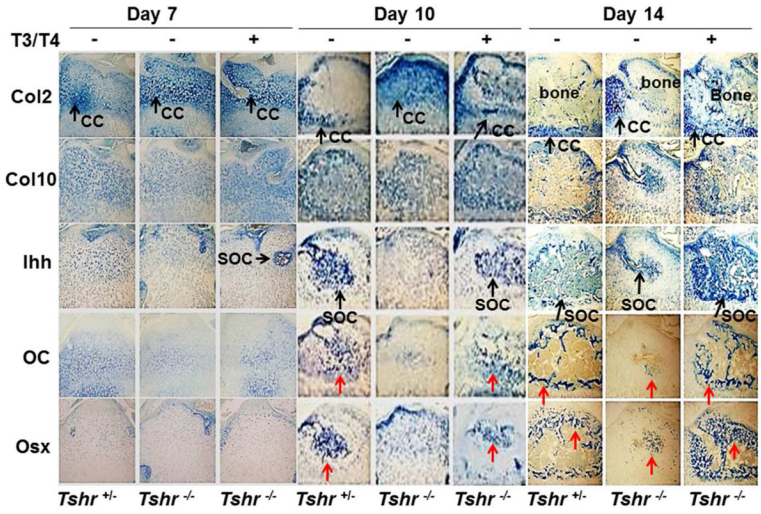

Figure 3. TH is essential for increased expression of Ihh, Osx, Col10 and OC in epiphyseal chondrocytes during SOC formation

Five consecutive sections were probed by immunohistochemistry for type 2 collagen (Col2), type 10 collagen (Col10), Ihh, osteocalcin (OC) and Osx in the epiphyses of vehicle treated *Tshr*$^{+/-}$, *Tshr*$^{-/-}$ and TH treated *Tshr*$^{-/-}$ mice at day 7, 10 and 14. Chondrogenic cells (CC), the secondary ossification center (SOC) and bone in the epiphyses of the tibias are labeled. Arrows in red indicate OC-positive and Osx-positive cells.

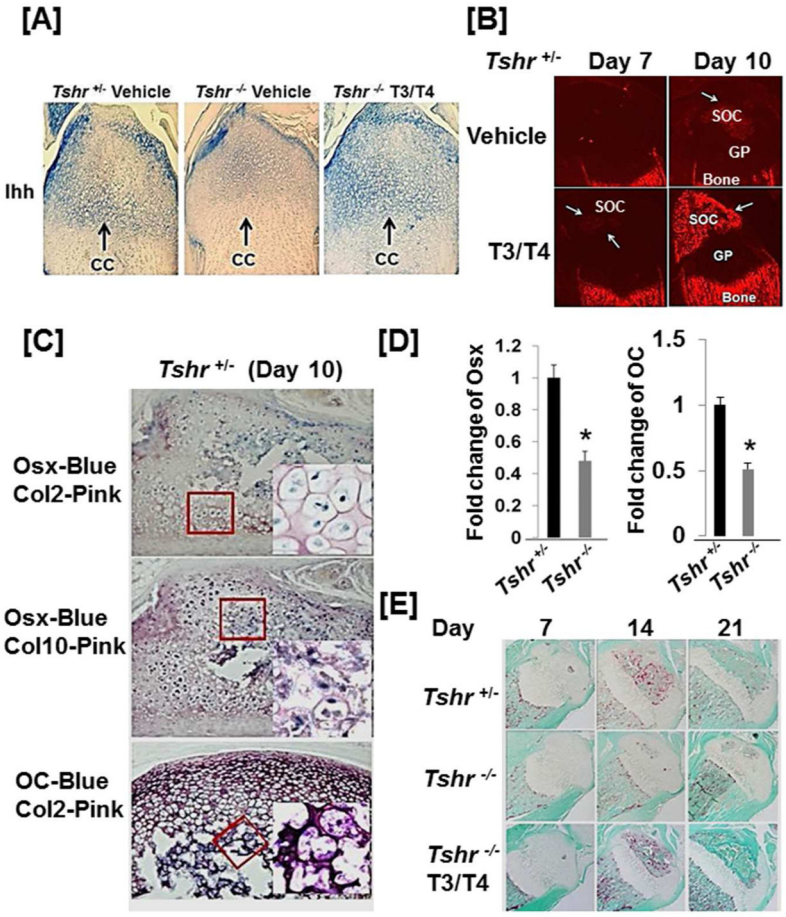

Figure 4. TH stimulates expression of Ihh and Osx to promote conversion of collagen 2 expressing chondrocytes into collagen 10/osteocalcin expressing chondro/osteoblasts

[**A**] Longitudinal sections of the epiphyses of the tibias of *Tshr*$^{+/-}$ control mouse and *Tshr*$^{-/-}$ mice at day 6 treated with T3/T4 or vehicle for 24 hours were probed by immunohistochemistry with anti-Ihh antibody. Arrows indicate chondrogenic cells (CC). **[B]** Osx-cherry reporter expression in the tibial epiphyses in Osx-cherry reporter mice treated twice with T3/T4 or vehicle at day 4 and 5. **[C]** Osx is co-expressed with Col2 and Col10 in chondro/osteoblast cells at the edge of the SOC. Consecutive sections of the tibias isolated from 10 day old *Tshr*$^{+/-}$ mice were double immunostained with Osx/Col2, Osx/Col10, and OC/Col2 antibodies, respectively. Areas in the highlighted boxes were visualized under high magnification (400x). **[D]** Osx and OC mRNA levels are reduced in the bones derived from *Tshr*$^{-/-}$ mice at day 10. The asterisk indicates a significant difference in *Tshr*$^{-/-}$ mice compared with the *Tshr*$^{+/-}$ littermate controls ($P < 0.01$). **[E]** Trap staining of the epiphyses of vehicle treated *Tshr*$^{+/-}$, *Tshr*$^{-/-}$ and TH treated *Tshr*$^{-/-}$ mice at day 7, 14 and 21.

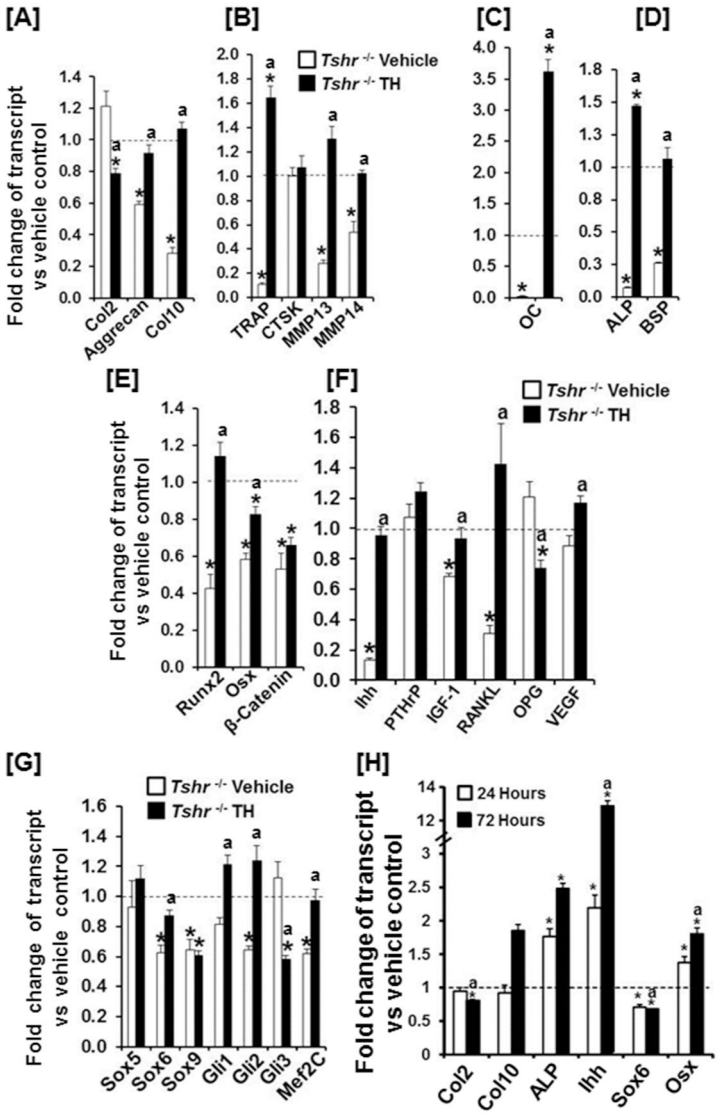

Figure 5. TH regulates expression levels of osteogenic markers, growth factors and transcription factors implicated in endochondral ossification

[A–H] Expression levels of chondrocyte differentiation markers [**A**], osteoclast differentiation and activity markers [**B**], osteoblast differentiation markers and transcription factors [**C–E**], growth factors [**F**], and chondrocyte differentiation transcription factors [**G**] in the epiphyses of vehicle treated $Tshr^{+/-}$, $Tshr^{-/-}$ and TH treated $Tshr^{-/-}$ mice at day 7. Values are expressed as fold change of expression level in $Tshr^{+/-}$ control mice. **An a**sterisk indicates a significant difference versus vehicle treated $Tshr^{+/-}$ mice ($P < 0.01$).). “a” indicates a significant difference compared to vehicle treated $Tshr^{-/-}$ mice ($P<0.01$). **[H]** Expression levels of Ihh, Osx and chondro/osteoblast markers in *in vitro* cultured epiphyses. Tibias derived from $Tshr^{+/-}$ mice were cultured *in vitro* in serum-free medium and in the presence or absence of 10 ng/ml of T3 for 24 hours and 72 hours. RNAs were extracted from tibial epiphyses for real-time RT-PCR. An asterisk indicates a significant difference in the epiphyses treated with T3 compared with bones treated with vehicle ($P < 0.01$). “a”

indicates a significant difference compared to 24 hours ($P<0.01$). TH regulates expression of growth factors and transcription factors in the epiphyseal chondrocytes to modulate cartilage degradation and bone formation.

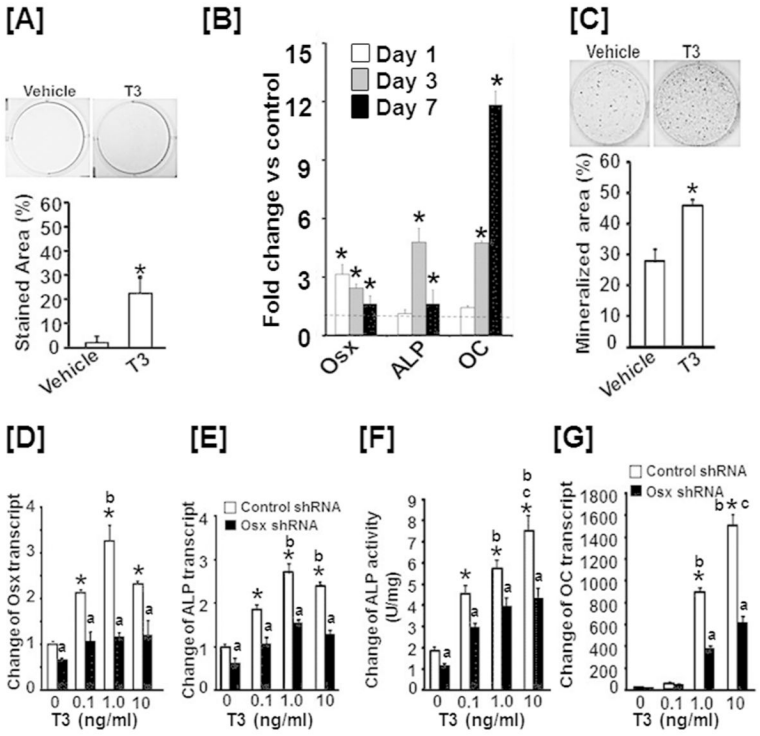

Figure 6. The TH effect on chondro/osteoblast differentiation is dependent on Osx expression

[A] T3 treatment increases ALP staining in ATDC5 cells. **[B]** TH stimulates expression of osteoblast markers in ATDC5 chondrogenic lineage cells. **[C]** T3 stimulates formation of mineralized nodules in ATDC5 cells. **[D–G]** Knockdown of Osx expression impairs chondrogenic cell differentiation into chondro/osteoblasts. ATDC5 cells were infected with lenti-virus expressing shRNA against Osx or GFP. The cells were then cultured in a serum-free medium with or without T3 for 24 hours prior to harvesting RNA for extraction and real time RT-PCR. Parallel cultures were also lysed for measurement of ALP activity. Values are expressed as fold change of vehicle treated ATDC5 cells transfected with GFP shRNA produced from lentivirus. An asterisk indicates a significant difference in T3 compared to vehicle treatment ($P < 0.01$). “a” indicates a significant difference in T3 treated ATDC5 cells transfected with GFP shRNA ($P<0.01$).). “b” indicates a significant difference compared to 0.1 ng/ml T3 treatment ($P<0.01$). “c” indicates a significant difference compared to 1 ng/ml T3 treatment ($P<0.01$).

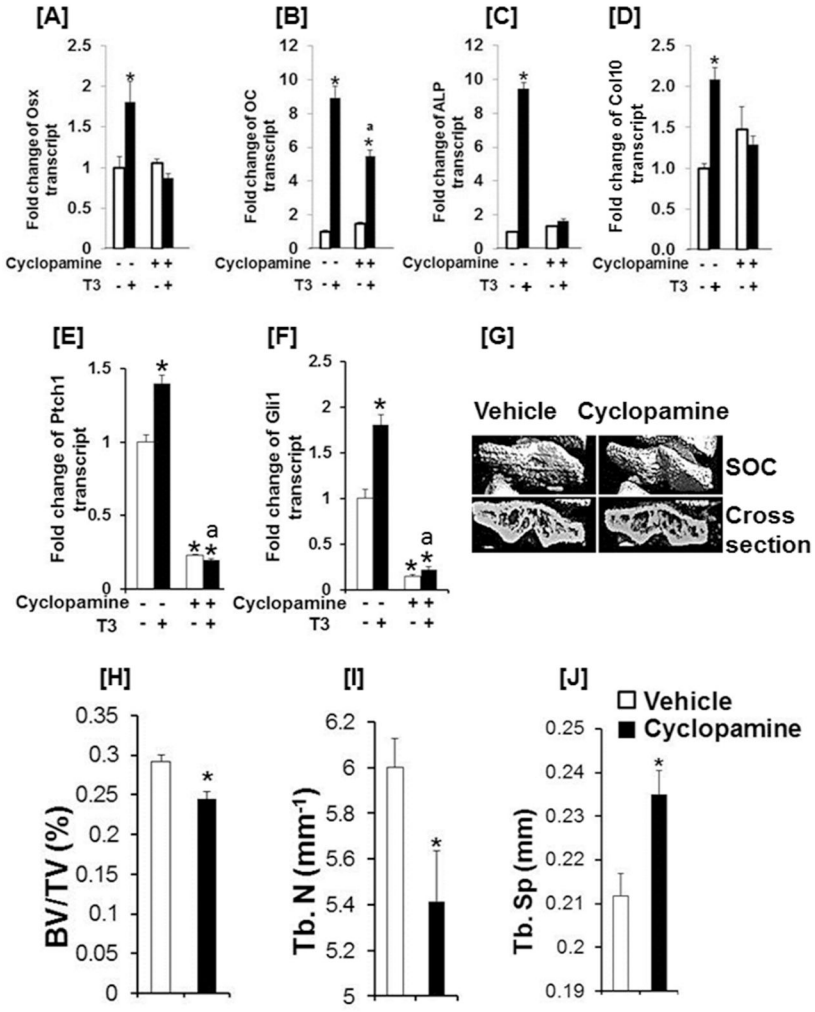

Figure 7. Blockade of Ihh signaling abolishes TH induction of Osx expression, chondro/osteoblast differentiation *in vitro* and SOC formation *in vivo*

[A–F] Cyclopamine treatment blocks the T3 effect on Osx, OC, ALP, Col10 mRNA, Ptch1, and Gli1 expression levels in epiphyseal chondrocytes. Tibia from 3 day old C57BL/6J mice were incubated with 10 ng/ml T3 or vehicle in the presence or absence of 10 μM cyclopamine for 72 h prior to RNA extraction in the epiphyses for real time RT-PCR. An asterisk indicates a significant difference compared to vehicle treated control epiphyses. "a" indicates a significant difference compared to T3 treated cultures without cyclopamine. **[G]** Representative micro-CT images of the tibia epiphyses isolated from *Tshr*$^{+/-}$ mice treated with vehicle or cyclopamine. *Tshr*$^{+/-}$ newborn mice were injected intraperitoneally with 2 mg/kg of cyclopamine daily for 10 days from day 5 to day 14 or the same volume of vehicle (5 mM NaOH). Mice were sacrificed and bones were isolated for micro-CT analyses at day 21. [**H–J**] Quantitative micro-CT data of the tibia epiphyses shown in E. Values are mean ± SEM (N = 5). An asterisk indicates a significant difference in vehicle treated compared to cyclopamine treated *Tshr*$^{+/-}$ mice (P<0.01).

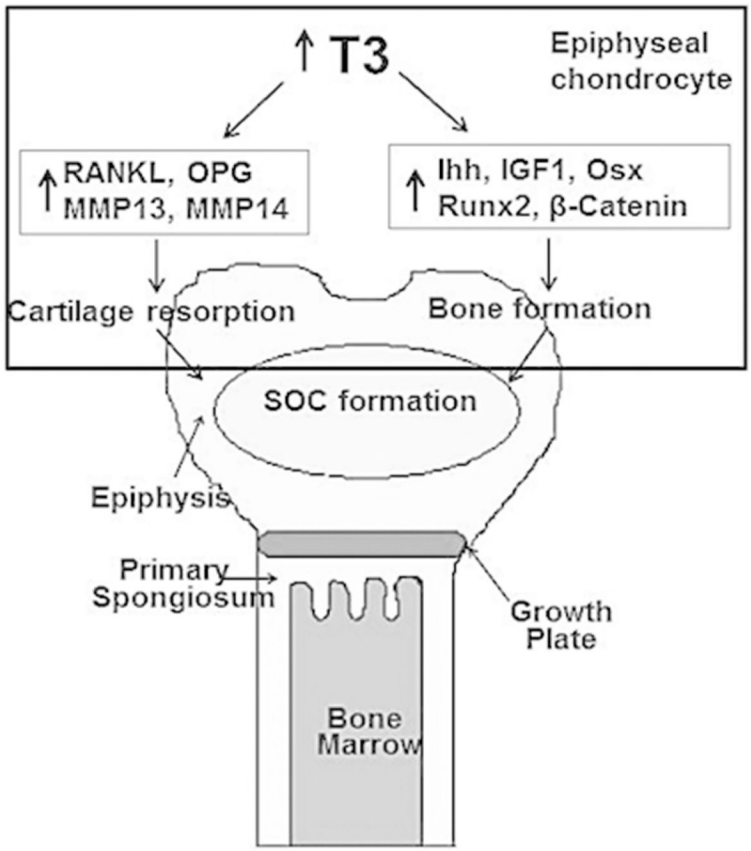

Figure 8.

A model of TH regulation of chondrocyte differentiation into chondro-osteoblasts (COB cells) to promote endochondral ossification in the epiphysis.